2018-05-24

A new in vitro assay measuring direct interaction of nonsense suppressors with the eukaryotic protein synthesis machinery

Martin Y. Ng
University of Pennsylvania

Et al.

A new *in vitro* assay measuring direct interaction of nonsense suppressors with the eukaryotic protein synthesis machinery

Martin Y. Ng[1], Haibo Zhang[1¥], Amy Weil[1†], Vijay Singh[2], Ryan Jamiolkowski[2], Alireza Baradaran-Heravi[3], Michel Roberge[3], Allan Jacobson[4], Westley Friesen[5], Ellen Welch[5], Yale E. Goldman[2], and Barry S. Cooperman[1*]

[1]Department of Chemistry, University of Pennsylvania, Philadelphia, PA 19104

[2]Department of Physiology, Perelman School of Medicine, University of Pennsylvania, Philadelphia, PA 19104

[3]Department of Biochemistry and Molecular Biology, University of British Columbia, Vancouver, BC, Canada V6T 1Z3

[4]Department of Microbiology and Physiological Systems, University of Massachusetts Medical School, Worcester, MA 01655

[5] PTC Therapeutics, 100 Corporate Court, South Plainfield, NJ 07080

* To whom to address inquiries

[¥] Present address: Spark Therapeutics, 3737 Market Street, Philadelphia, PA, 19104

[†] Present address: AdMed, Inc., 122 Union Square Drive, New Hope, PA, 18938

Abstract

Nonsense suppressors (NonSups) treat premature termination codon (PTC) disorders by inducing the selection of near cognate tRNAs at the PTC position, allowing readthrough of the PTC and production of full-length protein. Studies of NonSup-induced readthrough of eukaryotic PTCs have been carried out using animals, cells or crude cell extracts. In these studies, NonSups can promote readthrough directly, by binding to components of the protein synthesis machinery, or indirectly, by inhibiting nonsense-mediated mRNA decay or by other mechanisms. Here we utilize a highly-purified *in vitro* system (Zhang et al., 2016. *eLife* **5**: e13429) to measure exclusively direct NonSup-induced readthrough. Of 17 previously identified NonSups, 13 display direct effects, apparently via at least two different mechanisms. We can monitor such direct effects by single molecule FRET (smFRET). Future smFRET experiments will permit elucidation of the mechanisms by which NonSups stimulate direct readthrough, aiding ongoing efforts to improve the clinical usefulness of NonSups.

Introduction

Premature termination codons (PTCs) arise as a consequence of nonsense mutations and lead to the replacement of an amino acid codon in mRNA by one of three stop codons, UAA, UGA or UAG (Brenner, *et al.*, 1965; Shalev and Baasov, 2014; Keeling, *et al.*, 2014), resulting in inactive truncated protein products. Nonsense mutations constitute ~20% of transmitted or *de novo* germline mutations (Salvatori, *et al.*, 2009; Goldmann, *et al.*, 2012; Stenson, *et al.*, 2017). Globally, there are ~7000 genetically transmitted disorders in humans and ~11% of all human disease mutations are nonsense mutations (Loudon, 2013). Clearly, millions of people worldwide would benefit from effective therapies directed toward PTC suppression. Clinical trials have begun to evaluate the treatment of PTC disorders with therapeutic agents called nonsense suppressors (NonSups) (Peltz, *et al.*, 2013; McDonald, *et al.*, 2017; Zainal Abidin, *et al.*, 2017). NonSups induce the selection of near cognate tRNAs at the PTC position, and insertion of the corresponding amino acid into the nascent polypeptide, a process referred to as "readthrough", which restores the production of full length functional proteins, albeit at levels considerably reduced from wild-type. Even low rates of readthrough can improve clinical outcomes when essential proteins are completely absent. Examples of such essential proteins include Cystic Fibrosis Transmembrane Regulator (CFTR) (Brodlie, *et al.*, 2015), dystrophin, and the cancer tumor suppressors adenomatous polyposis coli (APS) (Floquet, *et al.*, 2011; Zilberberg, *et al.*, 2010) protein and p53 (Miyaki, *et al.*, 2002; Floquet, *et al.*, 2011; Roy, *et al.*, 2016; Baradaran-Heravi, *et al.*, 2016).

In vitro, ex vivo, and *in vivo* experiments and clinical trials have identified a diverse structural set of NonSups as candidates for PTC suppression therapy (Figure 1), including aminoglycosides (Shalev and Baasov, 2014; Bidou, *et al.*, 2017; Oishi, *et al.*, 2015; Duscha, *et al.*, 2014; Floquet, *et al.*, 2012; Sangkuhl, *et al.*, 2004; Fuchshuber-Moraes, *et al.*, 2011; Cogan, *et al.*,

2014; Baradaran-Heravi, *et al.*, 2017), ataluren (Peltz, *et al.*, 2013; Roy, *et al.*, 2016; Welch, *et al.*, 2007) and ataluren-like molecules (Du, *et al.*, 2009; Du, *et al.*, 2013; Gómez-Grau, *et al.*, 2015) and others (Zilberberg, *et al.*, 2010; Arakawa, *et al.*, 2003; Hamada, *et al.*, 2015; Caspi, *et al.*, 2016; Mutyam, *et al.*, 2016). To date, only one NonSup, ataluren (known commercially as Translarna), has been approved in the EU for clinical use, but this approval is limited to treatment of patients with nonsense-mediated Duchenne muscular dystrophy. The clinical utility of other NonSups, such as aminoglycosides, is restricted, in part, by their toxic side effects. A critical barrier to development of NonSups that are more clinically useful is the paucity of information regarding the precise mechanisms by which these molecules stimulate readthrough. All prior results measuring nonsense suppressor-induced readthrough (NSIRT) of eukaryotic PTCs have been carried out using animals, intact cells or crude cell extracts. In such systems, NonSups can promote readthrough directly, by binding to one or more of the components of the protein synthesis machinery, or indirectly, either by inhibiting nonsense-mediated mRNA decay (NMD) (He and Jacobson, 2015), or by modulating processes altering the cellular activity levels of protein synthesis machinery components (Feng, *et al.*, 2014; Keeling, 2016). These assays thus measure a quantity we define as TOTAL-NSIRT. This multiplicity of possible mechanisms of nonsense suppression within TOTAL-NSIRT has complicated attempts to determine the precise mechanisms of action of specific NonSups and limited the use of rational design in identifying new, more clinically useful NonSups.

Recently, we developed a highly purified, eukaryotic cell-free protein synthesis system (Zhang, *et al.*, 2016) that we apply here to examine the direct effects of the NonSups on the protein synthesis machinery, which we define as DIRECT-NSIRT. Our results allow us to distinguish NonSups acting directly on the protein synthesis machinery from those that act indirectly and

suggest that NonSups having DIRECT-NSIRT effects can be divided into at least two distinctive structural groups that induce nonsense suppression by different mechanisms. We also demonstrate the potential of using single molecule fluorescence resonance energy transfer (smFRET) experiments to elucidate the details of such mechanisms.

Materials and Methods

Nonsense suppressors (Figure 1). The following NonSups were obtained from commercial sources: gentamicin mixture and G418 (Sigma), nourseothricin sulfate, a mixture of streptothricins D and F (Gold Biotechnology), doxorubicin (Fisher Scientific), escin and tylosin (Alfa Aesar), azithromycin (APExBIO). Gentamicins B and B1 were prepared as described (Baradaran-Heravi, *et al.*, 2017). PTC Therapeutics supplied the following NonSups: ataluren sodium salt, RTC13, GJ071, GJ072, and gentamicin X2. Negamycin was a gift from Alexander Mankin, University of Illinois at Chicago. NB84 and NB124 (Bidou, *et al.*, 2017), currently available as ELX-02 and ELX-03, respectively, from Eloxx Pharmaceuticals (Waltham, MA), were gifts from Timor Baasov (Technion, Haifa).

Ribosomes and factors. Shrimp (*A. salina*) ribosome subunits were prepared from dried frozen commercial cysts as described (Zhang, *et al.*, 2016; Iwasaki and Kaziro, 1979) with slight modifications. Shrimp cysts (Pentair Aquatic Ecosystems) (425 g) were ground open using a blender in the presence of buffer M (30 mM HEPES-KOH, pH 7.5, 50 mM KCl, 10 mM $MgCl_2$, 8.5% mannitol, 0.5 mM EDTA, 2 mM DTT, 1 mM PMSF, 1:3000 RNasin (New England Biolabs) (500 mL), and two Protease Inhibitor Complete minitablets (Roche). Cyst debris was removed by two centrifugations at 30,000 x g for 15 min at 4°C. 80S ribosomes in the supernatant were

precipitated by adding 175 mL of 4.5% PEG 20k (Ben-Shem, *et al.*, 2011) and resuspended in 60 mL of dissociation buffer 1 (20 mM HEPES-KOH, pH 7.5, 500 mM KCl, 2 mM $MgCl_2$, 6.8% sucrose 2 mM DTT, 1:1000 RNasin, 2 protease minitablets). Puromycin was added to a final concentration of 2 mM, and the resulting solution was incubated on ice for 30 min, then at 37 °C for 15 min. 40S and 60S subunits (approximately 6,000 A_{260} units) were then resolved by a 10-30% hyperbolic sucrose gradient centrifugation for 16 h in a Beckman Ti15 zonal rotor at 376,000 x g in dissociation buffer 2 (20 mM HEPES, pH 7.5, 0.5 M KCl, 5 mM $MgCl_2$, 3 mM EDTA, 2 mM DTT) at 4 ^{o}C. Carrier 70S ribosomes were isolated from S30 of *E. coli* cells by three consecutive ultracentrifugations through a 1.1 M sucrose cushion in a buffer of 20 mM Tris, pH 7.5, 500 mM NH_4Cl, 10 mM Mg Acetate, 0.5 mM EDTA, 3 mM 2-mercaptoethanol. Elongation factors eEF2 (Jørgensen, *et al.*, 2002) and eEF1A (Thiele, *et al.*, 1985) were isolated from Baker's yeast as described. Yeast 6xHis-tagged release factors (full-length eRF1 and amino acids 166-685 of eRF3) were expressed in *E. coli* and purified using a TALON cobalt resin. Both release factors were a generous gift from Alper Celik (University of Massachusetts Medical School).

tRNA and mRNA. $tRNA^{Lys}$, $tRNA^{Val}$, $tRNA^{Gln}$, and $tRNA^{Met}$ were isolated from *E. coli* bulk tRNA (Roche). $tRNA^{Arg}$, $tRNA^{Trp}$ and $tRNA^{Leu}$ were isolated from Baker's yeast bulk tRNA (Roche), using hybridization with immobilized complementary oligoDNA as described previously (Barhoom, *et al.*, 2013; Liu, *et al.*, 2014). Yeast $tRNA^{Phe}$ (Sigma) and all isoacceptor tRNAs mentioned above where charged with their cognate amino acids as described (Pan, *et al.*, 2007; Pan, *et al.*, 2009). CrPV-IRES (Zhang, *et al.*, 2016) was modified by Genscript, Inc to encode the initial mRNA sequence UUCAAAGUGAGAUGGCUAAUG (denoted Trp-IRES). A point mutation was introduced into Trp-IRES to convert the UGG codon for Trp into a UGA stop codon

126 (UUCAAAGUGAGAUGACUAAUG, denoted Stop-IRES). These two sequences were inserted
127 into pUC57-Kan plasmid and amplified in TOP 10 competent cells. Plasmids were extracted using
128 QIAGEN Plasmid Kits and linearized. Trp-IRES and STOP-IRES were produced by in-vitro
129 transcription.
130
131 POST4 and POST5 Complex Preparation. 80S-IRES complex was first formed by incubating 0.8
132 μM 40S, 1.1 μM 60S and 0.8 μM IRES in Buffer 4 (40 mM Tris-HCl pH 7.5, 80 mM NH_4Cl, 5
133 mM $Mg(OAc)_2$, 100 mM KOAc, 3 mM 2-mercaptoethanol) at 37 °C for 2 min. Post-translocation
134 complex with FKVR-$tRNA^{Arg}$ in the ribosomal P-site tRNA (POST4) was formed by incubating
135 0.4 μM 80S-IRES with 0.4 μM each of the first four aminoacylated tRNAs, 0.4 μM eEF1A, 1.0
136 μM eEF2, 1 mM GTP at 37 °C for 25 min in Buffer 4. POST4 was then purified by
137 ultracentrifugation in 1.1 M sucrose with Buffer 4 at 540,000 x g for 90 min at 4°C. POST4 pellet
138 was resuspended in Buffer 4. Post-translocation complex with FKVRQ-$tRNA^{Gln}$ in the ribosomal
139 P-site tRNA (POST5) was prepared in identical fashion, except that the first five aminoacylated
140 tRNAs were added prior to the 25 min incubation at 37 °C. POST-4 amd POST-5 complexes could
141 be prepared and stored in small aliquots at -80 ^{0}C for at least three months with no discernible loss
142 of activity.
143
144 *In vitro* tRNA-Quant and PEP-Quant Readthrough Assays. POST5 complex (0.02 μM) was mixed
145 with Trp-$tRNA^{Trp}$, Leu-$tRNA^{Leu}$, and [^{35}S]-Met-$tRNA^{Met}$ (0.08 μM each), elongation factors
146 eEF1A (0.08 μM), eEF-2 (1.0 μM) and release factors eRF1 (0.010 μM) and eRF3 (0.020 μM)
147 and incubated at 37 °C in Buffer 4 for 20 min, in the absence or presence of NonSups.

For the tRNA-Quant Assay, reaction mixture aliquots (40 µL) were quenched with 150 µL of 0.5 M MES buffer (pH 6.0). Following addition of carrier 70S *E. coli* ribosomes (100 pmol, 3 µL of 33 µM 70S), all ribosomes were pelleted by ultracentrifugation through a 1.1 M sucrose solution in Buffer 4 (350 µL) at 540,000 x g for 70 min at 4°C. The ribosome pellet was resuspended in Buffer 4, and co-sedimenting FKVRQWL[^{35}S]M-tRNA^{Met} was determined.

For the Pep-Quant Assay, reaction mixture aliquots (80 µL) were quenched with 0.8 M KOH (9 µL of 8M KOH) and the base-quenched samples were incubated at 37 ^{o}C for 1 h to completely release octapeptide FKVRQWL[^{35}S]M from tRNA^{Met}. Acetic acid (9 µL) was then added to lower the pH to 2.8. Samples were next lyophilized, suspended in water, and centrifuged to remove particulates. The particulates contained no ^{35}S. The supernatant was analyzed by thin layer electrophoresis (TLE) as previously described (Youngman*, et al.*, 2004), using the same running buffer. The identity of FKVRQWLM was confirmed by the co-migration of the ^{35}S radioactivity with authentic samples obtained from GenScript (Piscataway, NJ). The ^{35}S radioactivity in the octapeptide band was used to determine the amount of octapeptide produced.

In both assays, the assay background was determined as ^{35}S either co-sedimenting (tRNA-Quant) or comigrating (PEP-Quant) in the absence of added Trp-tRNA^{Trp}. These levels were 0.09 ± 0.01 (sd, n = 80) octapeptide/POST5 for the tRNA-Quant assay and 0.04 ± 0.01 (sd, n = 8) octapeptide/POST5 for the PEP-Quant assay. Some NonSups are poorly soluble in water and were added to reaction mixtures from concentrated solutions made up in either DMSO (RTC13, GJ071, GJ072, azithromycin) or methanol (escin). The level of organic solvent in the assay medium was ≤ 0.5%. For these NonSups the small amount of readthrough induced in the presence of added Trp-tRNA^{Trp} by added organic solvent (Table S1) was additionally subtracted as background. Readthrough levels presented in Figures 3 and S3 are all background subtracted. Although PEP-

Quant has a lower procedural background, it is time consuming to perform, and less precise than tRNA-Quant. Both assays show a basal level of readthrough, in the absence of added NonSup, of 0.08 ± 0.02 (sd, n=40) octapeptide/POST5 above background, with some day-to-day variation.

smFRET experiments. Fluorescent ternary complexes (TCs) were prepared by incubating 1 μM eEF-1A, 3 μM GTP, and 1 μM charged tRNAs labeled with either Cy3 or Cy5 (Chen*, et al.*, 2011) at 37 °C for 15 min in Buffer 4. For experiments measuring only PRE6 complex formation, POST4 complex, containing FVKR-tRNA^{Arg} in the P-site and formed from ribosomes programmed with either Trp-IRES or Stop-IRES biotinylated at the 5' end (Chen*, et al.*, 2011), was incubated with 15 nM Gln-TC(Cy5), 1 μM eEF-2 and 2 mM GTP in buffer 4 for 5 min at room temperature. The resulting POST5 complex was immobilized on a streptavidin/biotin-PEG coated glass surface (Chen*, et al.*, 2011). After two minutes of incubation, unbound reaction components were washed out of the channel and 15 nM Trp-TC(Cy3) was added, with or without a NonSup, into the channel to make a PRE6 complex. Unbound Trp-TC(Cy3) was washed out of the channel with Buffer 4 containing a deoxygenation enzyme system of 100 μg/mL glucose oxidase, 3 mg/mL glucose, and 48 μg/mL catalase to minimize photobleaching. Cy3 and Cy5 fluorescence intensities were collected with 100 ms time resolution using alternating laser excitation (ALEX) between 532 nm and 640 nm lasers on an objective-type total internal reflection fluorescence microscope described previously (Chen*, et al.*, 2011). For experiments measuring both PRE6 complex and POST6 complex formation, Trp-IRES-PRE6 complex was formed as described above and 1 μM eEF-2 was injected while recording the FRET between FVKRQW-tRNA^{Trp}(Cy3) and tRNA^{Gln}(Cy5).

Ataluren ^{19}F NMR Spectroscopy. Various concentrations of ataluren solutions (0.03, 0.1 and 2.0 mM) were prepared in buffer 4 with 10% D_2O. The ^{19}F NMR spectrum of each solution was

recorded on a Bruker DMX 360 MHz NMR spectrometer with a 5 mm Quattro Nucleus Probe. Data were analyzed with mNova software.

Results

The *in vitro* ribosomal readthrough assay. Structural studies (Fernández, *et al.*, 2014; Koh, *et al.*, 2014; Muhs, *et al.*, 2015; Murray, *et al.*, 2016; Abeyrathne, *et al.*, 2016) have shown that, prior to polypeptide chain elongation, the cricket paralysis virus (CrPV) IRES structure occupies all three tRNA binding sites (E, P, and A) on the 80S ribosome. We have recently demonstrated that the first two cycles of peptide elongation proceed very slowly due to very low rates of pseudo-translocation and translocation, but that, following translocation of tripeptidyl-tRNA, subsequent elongation cycles proceed more rapidly (Zhang, *et al.*, 2016). Based on these results we constructed an assay to directly monitor readthrough of the sixth codon, when the faster elongation rate is well established. For this purpose, we prepared the two CrPv IRES coding sequences, STOP-IRES and Trp-IRES (Figure 2). STOP-IRES contains the stop codon UGA at position 6 and has a peptide coding sequence designed to give a high amount of readthrough, based on previous studies showing that readthrough at the UGA stop codon proceeds in higher yields than at either the UAA and UAG stop codons (Dabrowski, *et al.*, 2015) and that such readthrough is further increased by both a downstream CUA codon (encoding Leu) at positions +4 - +6 (Stiebler, *et al.*, 2014; Loughran, *et al.*, 2014) and an upstream AA sequence at positions -1 and -2 (Dabrowski, *et al.*, 2015). In TRP-IRES UGA is replaced by UGG which is cognate to $tRNA^{Trp}$, the most efficient natural tRNA suppressor of the UGA codon (Blanchet, *et al.*, 2014; Roy, *et al.*, 2015). Trp-IRES encodes the octapeptide FKVRQWLM, which permits facile quantification of octapeptide synthesis by ^{35}S-Met incorporation.

For the results reported below, we first prepared two POST5 translocation complexes, each containing FKVRQ-tRNA^{Gln} in the P-site, using ribosomes programmed with either STOP-IRES or TRP-IRES. We then used the tRNA-Quant assay, which is rapid and precise, to determine the amount of FKVRQWLM-tRNA^{Met} formed on incubating each POST5 complex with a mixture of Trp-tRNA^{Trp}, Leu-tRNA^{Leu}, [^{35}S]-Met-tRNA^{Met}, elongation factors eEF1A and eEF2 and release factors eRF1 and eRF3. We verified the validity of the tRNA-Quant assay by demonstrating that it gives results that are very similar to those obtained with the PEP-Quant assay (Figure S1), in which, following base treatment, the amount of FKVRQWLM octapeptide is determined following a TLE separation procedure (Zhang, *et al.*, 2016; Youngman, *et al.*, 2004).

Induction of readthrough by aminoglycosides (AGs). Results with the eight AGs examined are all consistent with a single tight site of AG binding to the ribosome (Garreau de Loubresse, *et al.*, 2014) resulting in increased readthrough, with EC_{50}s falling in the range of 0.14 – 4 μM and fractional readthrough efficiencies of Stop-IRES varying from 0.1 – 0.3 (Table 1), as compared with an efficiency of 1.00 ± 0.02 (n = 24) for conversion of POST5 to POST8 complex with Trp-IRES (Figure 3A, Table 1). These results are consistent with results on readthrough obtained in intact cells showing a) G418, gentamicin B1 (Baradaran-Heravi, *et al.*, 2017), NB84, NB124 (Bidou, *et al.*, 2017) and gentamicin X2 (Friesen, *et al.*, 2018) to be much more effective than the gentamicin mixture currently used as an approved antibiotic; b) gentamicin B1 to be much more effective than gentamicin B, despite their differing by only a single methyl group (Figure 1) (Baradaran-Heravi, *et al.*, 2017); c) gentamicin B1 to be more effective than streptothricin (Figure S2C); d) NB84, NB124 (Bidou, *et al.*, 2017), and gentamicin X2 (Friesen, *et al.*, 2018), to have similar potencies, measured by either EC_{50} or readthrough efficiency.

Induction of readthrough by ataluren-like compounds. The NonSups ataluren, GJ072, and RTC 13 share similar structures, containing a central aromatic heterocycle having two or three substituents, at least one of which is aromatic (Figure 1). They also show similar S-shaped readthrough activity saturation curves (Figure 3B), with EC_{50} values between 0.17 – 0.35 mM and plateau readthrough efficiencies ranging from 0.10 – 0.16 (Table 1). These S-shaped curves yield Hill n values of ~ 4, which suggest multi-site binding of ataluren-like NonSups to the protein synthesis machinery. Formation of NonSup aggregates in solution that induce readthrough could also give rise to S-shaped curves, but we consider this to be unlikely based on the constancy of the chemical shift and line shape of ataluren's ^{19}F NMR peak over a concentration range of 0.03 – 2.0 mM (see Supplementary Information).

Induction of readthrough by other NonSups. Two other reported NonSups, negamycin (Taguchi, *et al.*, 2017) and doxorubicin (Mutyam, *et al.*, 2016) also display readthrough activity in the tRNA-Quant assay (Figure 3B). The results with each fit a simple saturation curve. Both NonSups have similar readthrough efficiencies (0.10 – 0.13) but a 50-fold difference in EC_{50} values, with doxorubicin having the much lower value (Table 1). Several other compounds that have readthrough activity in cellular assays, tylosin (Zilberberg, *et al.*, 2010), azithromycin (Caspi, *et al.*, 2016), GJ071 (Du, *et al.*, 2013) and escin (Mutyam, *et al.*, 2016) showed little or no activity in the tRNA-Quant assay in the concentration range 30 – 600 μM (Figure S3). In addition, escin at high concentration inhibits both basal readthrough elongation and normal elongation, the latter measured with Trp-IRES programmed ribosomes, with the effect on basal readthrough being much more severe (Figure S4).

263 Single molecule assay of readthrough activity. Two fluorescent labeled tRNAs, when bound
264 simultaneously to a ribosome, at either the A- and P-sites in a pretranslocation complex, or the P-
265 and E-sites in a posttranslocation complex, are close enough to generate a FRET signal (Chen, *et*
266 *al.*, 2011; Blanchard, *et al.*, 2004). We observed tRNA-tRNA FRET in the pretranslocation
267 complex (Trp-IRES-PRE6), formed by incubating the Cy5-labeled Trp-IRES-POST5 with Cy3-
268 labeled eEF1A.GTP.Trp-tRNA^{Trp}, and having tRNA^{Gln}(Cy5) in the P-site and FKVRQW-
269 tRNA^{Trp}(Cy3) in the A-site (Figure 4). Addition of eEF2.GTP converted Trp-IRES-PRE6 to a Trp-
270 IRES-POST6 complex, containing tRNA^{Gln}(Cy5) in the E-site and FKVRQW-tRNA^{Trp}(Cy3) in
271 the P-site, which is accompanied by an increase in Cy3:Cy5 FRET efficiency (Figure 4).
272 Repetition of this experiment with Stop-IRES-POST5 in the absence of eEF2 decreased the
273 number of pretranslocation complexes (STOP-IRES-PRE6) formed to 24% of that seen with Trp-
274 IRES (Figure 4). This value was increased in a dose-dependent manner by addition of either G418
275 or gentamicin B1 (Figure 4B), with relative potencies similar to those displayed in Table 1. G418
276 and gentamicin did not significantly affect formation of Trp-IRES-PRE6 from Trp-IRES-POST5
277 on addition of Cy3-labeled eEF1A.GTP.Trp-tRNA^{Trp}. The agreement between the ensemble and
278 single molecule assays demonstrates our ability to monitor NonSup-induced readthrough by
279 smFRET, which, in subsequent studies, will allow determination of the effects of NonSups on the
280 dynamics of the nascent peptide elongation cycle that commences with suppressor tRNA
281 recognition of a premature stop codon.
282
283 **Discussion**
284 Here we utilize a straightforward *in vitro* assay, tRNA-Quant, to measure direct nonsense
285 suppressor-induced readthrough (DIRECT-NSIRT) of a termination codon. In the tRNA-Quant
286 assay, the arrival of the UGA termination codon into the 40S subunit portion of the tRNA A-site

has two possible outcomes: termination of peptide synthesis via eRF1/eRF3-catayzed hydrolysis of the P-site-bound FKVRQ-tRNA^{Gln} or readthrough via productive A-site binding of near-cognate Trp-tRNA^{Trp} followed by productive binding of the cognate Leu-tRNA^{Leu} and Met- tRNA^{Met} leading to FKVRQWLM-tRNA^{Met} formation. NonSups increase the readthrough percentage by binding to one or more of the specific components of the protein synthesis apparatus present in the assay. Our working hypothesis is that Direct-NSIRT is an important, perhaps dominant, part of Total-NSIRT for NonSups showing parallel effects in tRNA-Quant and cellular assays, such as those included in Table 1. In contrast, biological activities of NonSups showing strong readthrough activity in cellular assays but little readthrough activity in tRNA-Quant (Figure S3), are likely be dominated by indirect effects.

Our results suggest that aminoglycosides and ataluren-like compounds stimulate readthrough by different mechanisms, AGs via binding to a single tight site on the ribosome and ataluren-like compounds via weaker, multi-site binding. (Figures 3, S2; Table 1). The EC_{50} values found in intact cells differ considerably from those measured by tRNA-Quant, being much higher for AGs (Bidou*, et al.*, 2017; Baradaran-Heravi*, et al.*, 2017), and much lower for ataluren (Peltz*, et al.*, 2013; Roy*, et al.*, 2016), RTC13 (Du*, et al.*, 2013) and GJ072 (Du*, et al.*, 2013). We attribute these differences to the fact that positively charged aminoglycosides are taken up poorly into cells, while uptake is favored for the hydrophobic ataluren-like molecules. Thus, vis-à-vis the culture medium, intracellular concentration would be expected to be lower for AGs and higher for ataluren, RTC13 and GJ072. Although the NonSups doxorubicin and negamycin have only modest activities (Figure 3, Table 1) each of these compounds have potential interest for future development. Doxorubicin has a relatively low EC_{50}, is clinically approved for use in cancer chemotherapy, and is the subject of ongoing efforts to identify doxorubicin congeners having

lower toxicity than doxorubicin itself (Kizek, *et al.*, 2012; Edwardson, *et al.*, 2015). Negamycin exhibits low acute toxicity and there are ongoing efforts to increase its readthrough activity via structure – function studies (Taguchi, *et al.*, 2017).

A critical barrier to further development of NonSups that are clinically useful is the paucity of information regarding the mechanisms by which they stimulate readthrough and misreading. Aminoglycosides have well-characterized binding sites in both prokaryotic (Lin, *et al.*, 2018) and eukaryotic ribosomes (Garreau de Loubresse, *et al.*, 2014), proximal to the small subunit decoding center, that have been linked to their promotion of misreading. Similarly, the functionally important prokaryotic ribosome binding site of negamycin has also been identified within a conserved small subunit rRNA region that is proximal to the decoding center (Lin, *et al.*, 2018; Spahn, *et al.*, 2001), and it is not unlikely that this site is also present in eukaryotic ribosomes. However, nothing is known about the readthrough-inducing sites of action within the protein synthesis apparatus of the ataluren-like NonSups (Figure 3B) or of doxorubicin. Indeed, it has even been suggested that ataluren may not target the ribosome (Pibiri, *et al.*, 2015). Although aminoglycosides have been the subject of detailed mechanism studies of their effects on prokaryotic misreading (Liu, *et al.*, 2014; Pape, *et al.*, 2000; Gromadski and Rodnina, 2004; Cochella, *et al.*, 2006; Tsai, *et al.*, 2013; Zhang, *et al.*, 2018), questions remain over their precise modes of action, and detailed mechanistic studies on aminoglycoside stimulation of eukaryotic readthrough and misreading are completely lacking. Virtually nothing is known about the mechanisms of action of negamycin, doxorubicin, and the ataluren-like NonSups in stimulating eukaryotic readthrough. Single molecule FRET is a method of choice for obtaining detailed information about processive biochemical reaction mechanisms (Roy, *et al.*, 2008), particularly in the study of protein synthesis (Perez and Gonzalez, 2011; Aitken, *et al.*, 2010; Wang, *et al.*, 2011;

333 Chen, *et al.*, 2013), because it permits determination of distributions, variations and fluctuations
334 among different ribosome conformational states and of complex multistep reaction trajectories.
335 Here we demonstrate the feasibility of using smFRET observations for detailed examination of
336 NonSup-stimulation of readthrough (Figure 4) and misreading, which, combined with other
337 mechanistic studies, should aid in achieving the understanding needed to improve the clinical
338 usefulness of NonSups.
339

340 **Acknowledgements**

341 We thank Drs. Alexander Mankin (University of Illinois at Chicago), Timor Baasov (Technion,
342 Haifa) and Alper Celik (University of Massachusetts Medical School) for reagents used in these
343 studies and Carla Zimmerman for technical assistance. This work was supported by research grants
344 to BSC from PTC Therapeutics and the Orphan Disease Center, University of Pennsylvania
345 (MDBR-17-108-CF1282X), to YEG (NIH GM118139), to MR (Michael Smith Foundation for
346 Health Research) and AJ (NIH GM27757 and GM122468).

References

1 Brenner, S., Stretton, A. O. W. & Kaplan, S. 1965. Genetic Code: The 'Nonsense' Triplets for Chain Termination and their Suppression. *Nature* **206**: 994, doi:10.1038/206994a0.

2 Shalev, M. & Baasov, T. 2014. When Proteins Start to Make Sense: Fine-tuning Aminoglycosides for PTC Suppression Therapy. *MedChemComm* **5**: 1092-1105, doi:10.1039/C4MD00081A.

3 Keeling, K. M., Xue, X., Gunn, G. & Bedwell, D. M. 2014. Therapeutics Based on Stop Codon Readthrough. *Annu. Rev. Genom. Hum. Genet.* **15**: 371-394, doi:10.1146/annurev-genom-091212-153527.

4 Salvatori, F. *et al.* 2009. Production of β-globin and adult hemoglobin following G418 treatment of erythroid precursor cells from homozygous β(0)39 thalassemia patients. *Am. J. Hematol.* **84**: 720-728, doi:10.1002/ajh.21539.

5 Goldmann, T., Overlack, N., Möller, F., Belakhov, V., van Wyk, M., Baasov, T., Wolfrum, U. & Nagel-Wolfrum, K. 2012. A comparative evaluation of NB30, NB54 and PTC124 in translational read-through efficacy for treatment of an USH1C nonsense mutation. *EMBO Molecular Medicine* **4**: 1186-1199, doi:10.1002/emmm.201201438.

6 Stenson, P. D., Mort, M., Ball, E. V., Evans, K., Hayden, M., Heywood, S., Hussain, M., Phillips, A. D. & Cooper, D. N. 2017. The Human Gene Mutation Database: towards a comprehensive repository of inherited mutation data for medical research, genetic diagnosis and next-generation sequencing studies. *Hum. Genet.* **136**: 665-677, doi:10.1007/s00439-017-1779-6.

7 Loudon, J. A. 2013. Repurposing amlexanox as a 'run the red light cure- all' with read-through – a 'no-nonsense' approach to eersonalised medicine. *J. Bioanal. Biomed.* **5**: 079-096, doi:doi: 10.4172/1948-593X.1000086.

8 Peltz, S. W., Morsy, M., Welch, E. M. & Jacobson, A. 2013. Ataluren as an Agent for Therapeutic Nonsense Suppression. *Annu. Rev. Med.* **64**: 407-425, doi:10.1146/annurev-med-120611-144851.

9 McDonald, C. M. *et al.* 2017. Ataluren in patients with nonsense mutation Duchenne muscular dystrophy (ACT DMD): a multicentre, randomised, double-blind, placebo-controlled, phase 3 trial. *Lancet* **390**: 1489-1498, doi:10.1016/S0140-6736(17)31611-2.

10 Zainal Abidin, N., Haq, I. J., Gardner, A. I. & Brodlie, M. 2017. Ataluren in cystic fibrosis: development, clinical studies and where are we now? *Expert Opin. Pharmacother.* **18**: 1363-1371, doi:10.1080/14656566.2017.1359255.

11 Brodlie, M., Haq, I. J., Roberts, K. & Elborn, J. S. 2015. Targeted therapies to improve CFTR function in cystic fibrosis. *Genome Med.* **7**: 101, doi:10.1186/s13073-015-0223-6.

12 Floquet, C., Rousset, J.-P. & Bidou, L. 2011. Readthrough of Premature Termination Codons in the Adenomatous Polyposis Coli Gene Restores Its Biological Activity in Human Cancer Cells. *PLoS One* **6**: e24125, doi:10.1371/journal.pone.0024125.

13 Zilberberg, A., Lahav, L. & Rosin-Arbesfeld, R. 2010. Restoration of APC gene function in colorectal cancer cells by aminoglycoside- and macrolide-induced read-through of premature termination codons. *Gut* **59**: 496-507, doi:10.1136/gut.2008.169805.

14 Miyaki, M., Iijima, T., Yasuno, M., Kita, Y., Hishima, T., Kuroki, T. & Mori, T. 2002. High incidence of protein-truncating mutations of the p53 gene in liver metastases of colorectal carcinomas. *Oncogene* **21**: 6689, doi:10.1038/sj.onc.1205887.

15 Floquet, C., Deforges, J., Rousset, J.-P. & Bidou, L. 2011. Rescue of non-sense mutated p53 tumor suppressor gene by aminoglycosides. *Nucleic Acids Res.* **39**: 3350-3362, doi:10.1093/nar/gkq1277.

16 Roy, B. *et al.* 2016. Ataluren stimulates ribosomal selection of near-cognate tRNAs to promote nonsense suppression. *Proc. Natl. Acad. Sci. USA* **113**: 12508-12513, doi:10.1073/pnas.1605336113.

17 Baradaran-Heravi, A. *et al.* 2016. Novel small molecules potentiate premature termination codon readthrough by aminoglycosides. *Nucleic Acids Res.* **44**: 6583-6598, doi:10.1093/nar/gkw638.

18 Bidou, L., Bugaud, O., Belakhov, V., Baasov, T. & Namy, O. 2017. Characterization of new-generation aminoglycoside promoting premature termination codon readthrough in cancer cells. *RNA Biol.* **14**: 378-388, doi:10.1080/15476286.2017.1285480.

19 Oishi, N. *et al.* 2015. XBP1 mitigates aminoglycoside-induced endoplasmic reticulum stress and neuronal cell death. *Cell Death Dis.* **6**: e1763, doi:10.1038/cddis.2015.108.

20 Duscha, S. *et al.* 2014. Identification and Evaluation of Improved 4′-O-(Alkyl) 4,5-Disubstituted 2-Deoxystreptamines as Next-Generation Aminoglycoside Antibiotics. *mBio* **5**, doi:10.1128/mBio.01827-14.

21 Floquet, C., Hatin, I., Rousset, J.-P. & Bidou, L. 2012. Statistical Analysis of Readthrough Levels for Nonsense Mutations in Mammalian Cells Reveals a Major Determinant of Response to Gentamicin. *PLoS Genet.* **8**: e1002608, doi:10.1371/journal.pgen.1002608.

22 Sangkuhl, K., Schulz, A., Römpler, H., Yun, J., Wess, J. & Schöneberg, T. 2004. Aminoglycoside-mediated rescue of a disease-causing nonsense mutation in the V2 vasopressin receptor gene in vitro and in vivo. *Hum. Mol. Genet.* **13**: 893-903, doi:10.1093/hmg/ddh105.

23 Fuchshuber-Moraes, M., Sampaio Carvalho, R., Rimmbach, C., Rosskopf, D., Alex Carvalho, M. & Suarez-Kurtz, G. 2011. Aminoglycoside-induced suppression of

CYP2C19*3 premature stop codon. *Pharmacogenet. Genomics* **21**: 694-700, doi:10.1097/FPC.0b013e328349daba.

24 Cogan, J., Weinstein, J., Wang, X., Hou, Y., Martin, S., South, A. P., Woodley, D. T. & Chen, M. 2014. Aminoglycosides Restore Full-length Type VII Collagen by Overcoming Premature Termination Codons: Therapeutic Implications for Dystrophic Epidermolysis Bullosa. *Mol. Ther.* **22**: 1741-1752, doi:doi.org/10.1038/mt.2014.140.

25 Baradaran-Heravi, A. *et al.* 2017. Gentamicin B1 is a minor gentamicin component with major nonsense mutation suppression activity. *Proc. Natl. Acad. Sci. USA* **114**: 3479-3484, doi:10.1073/pnas.1620982114.

26 Welch, E. M. *et al.* 2007. PTC124 targets genetic disorders caused by nonsense mutations. *Nature* **447**: 87, doi:10.1038/nature05756.

27 Du, L. *et al.* 2009. Nonaminoglycoside compounds induce readthrough of nonsense mutations. *J. Exp. Med.* **206**: 2285-2297, doi:10.1084/jem.20081940.

28 Du, L. *et al.* 2013. A New Series of Small Molecular Weight Compounds Induce Read Through of All Three Types of Nonsense Mutations in the ATM Gene. *Mol. Ther.* **21**: 1653-1660, doi:10.1038/mt.2013.150.

29 Gómez-Grau, M. *et al.* 2015. Evaluation of Aminoglycoside and Non-Aminoglycoside Compounds for Stop-Codon Readthrough Therapy in Four Lysosomal Storage Diseases. *PLoS One* **10**: e0135873, doi:10.1371/journal.pone.0135873.

30 Arakawa, M. *et al.* 2003. Negamycin Restores Dystrophin Expression in Skeletal and Cardiac Muscles of *mdx* Mice. *J. Biochem.* **134**: 751-758, doi:10.1093/jb/mvg203.

31 Hamada, K., Taguchi, A., Kotake, M., Aita, S., Murakami, S., Takayama, K., Yakushiji, F. & Hayashi, Y. 2015. Structure–Activity Relationship Studies of 3-epi-Deoxynegamycin Derivatives as Potent Readthrough Drug Candidates. *ACS Med. Chem. Lett.* **6**: 689-694, doi:10.1021/acsmedchemlett.5b00121.

32 Caspi, M. *et al.* 2016. A flow cytometry-based reporter assay identifies macrolide antibiotics as nonsense mutation read-through agents. *J. Mol. Med.* **94**: 469-482, doi:10.1007/s00109-015-1364-1.

33 Mutyam, V. *et al.* 2016. Discovery of Clinically Approved Agents That Promote Suppression of Cystic Fibrosis Transmembrane Conductance Regulator Nonsense Mutations. *Am. J. Respir. Crit. Care Med.* **194**: 1092-1103, doi:10.1164/rccm.201601-0154OC.

34 He, F. & Jacobson, A. 2015. Nonsense-Mediated mRNA Decay: Degradation of Defective Transcripts Is Only Part of the Story. *Annu. Rev. Genet.* **49**: 339-366, doi:10.1146/annurev-genet-112414-054639.

35 Feng, T. *et al.* 2014. Optimal Translational Termination Requires C4 Lysyl Hydroxylation of eRF1. *Mol. Cell* **53**: 645-654, doi:10.1016/j.molcel.2013.12.028.

36 Keeling, K. M. 2016. Nonsense Suppression as an Approach to Treat Lysosomal Storage Diseases. *Diseases* **4**: 32, doi:10.3390/diseases4040032.

37 Zhang, H., Ng, M. Y., Chen, Y. & Cooperman, B. S. 2016. Kinetics of initiating polypeptide elongation in an IRES-dependent system. *eLife* **5**: e13429, doi:10.7554/eLife.13429.

38 Iwasaki, K. & Kaziro, Y. 1979. [60] Polypeptide chain elongation factors from pig liver. Moldave, K. & L. Grossman, editors. *Methods Enzymol.* New York: Academic Press, **60**: 657-676.

39 Ben-Shem, A., Garreau de Loubresse, N., Melnikov, S., Jenner, L., Yusupova, G. & Yusupov, M. 2011. The Structure of the Eukaryotic Ribosome at 3.0 Å Resolution. *Science* **334**: 1524-1529, doi:10.1126/science.1212642.

40 Jørgensen, R., Carr-Schmid, A., Ortiz, P. A., Kinzy, T. G. & Andersen, G. R. 2002. Purification and crystallization of the yeast elongation factor eEF2. *Acta Crystallogr. Sect. D. Biol. Crystallogr.* **58**: 712-715, doi:doi:10.1107/S0907444902003001.

41 Thiele, D., Cottrelle, P., Iborra, F., Buhler, J. M., Sentenac, A. & Fromageot, P. 1985. Elongation factor 1 alpha from Saccharomyces cerevisiae. Rapid large-scale purification and molecular characterization. *J. Biol. Chem.* **260**: 3084-3089.

42 Barhoom, S., Farrell, I., Shai, B., Dahary, D., Cooperman, B. S., Smilansky, Z., Elroy-Stein, O. & Ehrlich, M. 2013. Dicodon monitoring of protein synthesis (DiCoMPS) reveals levels of synthesis of a viral protein in single cells. *Nucleic Acids Res.* **41**: e177-e177, doi:10.1093/nar/gkt686.

43 Liu, J. *et al.* 2014. Monitoring Collagen Synthesis in Fibroblasts Using Fluorescently Labeled tRNA Pairs. *J. Cell. Physiol.* **229**: 1121-1129, doi:doi:10.1002/jcp.24630.

44 Pan, D., Kirillov, S. V. & Cooperman, B. S. 2007. Kinetically Competent Intermediates in the Translocation Step of Protein Synthesis. *Mol. Cell* **25**: 519-529, doi:10.1016/j.molcel.2007.01.014.

45 Pan, D., Qin, H. & Cooperman, B. S. 2009. Synthesis and functional activity of tRNAs labeled with fluorescent hydrazides in the D-loop. *RNA* **15**: 346-354, doi:10.1261/rna.1257509.

46 Youngman, E. M., Brunelle, J. L., Kochaniak, A. B. & Green, R. 2004. The Active Site of the Ribosome Is Composed of Two Layers of Conserved Nucleotides with Distinct Roles in Peptide Bond Formation and Peptide Release. *Cell* **117**: 589-599, doi:10.1016/S0092-8674(04)00411-8.

47 Chen, C. *et al.* 2011. Single-Molecule Fluorescence Measurements of Ribosomal Translocation Dynamics. *Mol. Cell* **42**: 367-377, doi:10.1016/j.molcel.2011.03.024.

48 Fernández, Israel S., Bai, X.-C., Murshudov, G., Scheres, Sjors H. W. & Ramakrishnan, V. 2014. Initiation of Translation by Cricket Paralysis Virus IRES Requires Its Translocation in the Ribosome. *Cell* **157**: 823-831, doi:10.1016/j.cell.2014.04.015.

49 Koh, C. S., Brilot, A. F., Grigorieff, N. & Korostelev, A. A. 2014. Taura syndrome virus IRES initiates translation by binding its tRNA-mRNA–like structural element in the ribosomal decoding center. *Proc. Natl. Acad. Sci. USA* **111**: 9139-9144, doi:10.1073/pnas.1406335111.

50 Muhs, M., Hilal, T., Mielke, T., Skabkin, Maxim A., Sanbonmatsu, Karissa Y., Pestova, Tatyana V. & Spahn, Christian M. T. 2015. Cryo-EM of Ribosomal 80S Complexes with Termination Factors Reveals the Translocated Cricket Paralysis Virus IRES. *Mol. Cell* **57**: 422-432, doi:10.1016/j.molcel.2014.12.016.

51 Murray, J., Savva, C. G., Shin, B.-S., Dever, T. E., Ramakrishnan, V. & Fernández, I. S. 2016. Structural characterization of ribosome recruitment and translocation by type IV IRES. *eLife* **5**: e13567, doi:10.7554/eLife.13567.

52 Abeyrathne, P. D., Koh, C. S., Grant, T., Grigorieff, N. & Korostelev, A. A. 2016. Ensemble cryo-EM uncovers inchworm-like translocation of a viral IRES through the ribosome. *eLife* **5**: e14874, doi:10.7554/eLife.14874.

53 Dabrowski, M., Bukowy-Bieryllo, Z. & Zietkiewicz, E. 2015. Translational readthrough potential of natural termination codons in eucaryotes – The impact of RNA sequence. *RNA Biol.* **12**: 950-958, doi:10.1080/15476286.2015.1068497.

54 Stiebler, A. C., Freitag, J., Schink, K. O., Stehlik, T., Tillmann, B. A. M., Ast, J. & Bölker, M. 2014. Ribosomal Readthrough at a Short UGA Stop Codon Context Triggers Dual Localization of Metabolic Enzymes in Fungi and Animals. *PLoS Genet.* **10**: e1004685, doi:10.1371/journal.pgen.1004685.

55 Loughran, G., Chou, M.-Y., Ivanov, I. P., Jungreis, I., Kellis, M., Kiran, A. M., Baranov, P. V. & Atkins, J. F. 2014. Evidence of efficient stop codon readthrough in four mammalian genes. *Nucleic Acids Res.* **42**: 8928-8938, doi:10.1093/nar/gku608.

56 Blanchet, S., Cornu, D., Argentini, M. & Namy, O. 2014. New insights into the incorporation of natural suppressor tRNAs at stop codons in Saccharomyces cerevisiae. *Nucleic Acids Res.* **42**: 10061-10072, doi:10.1093/nar/gku663.

57 Roy, B., Leszyk, J. D., Mangus, D. A. & Jacobson, A. 2015. Nonsense suppression by near-cognate tRNAs employs alternative base pairing at codon positions 1 and 3. *Proc. Natl. Acad. Sci. USA* **112**: 3038-3043, doi:10.1073/pnas.1424127112.

525 58 Garreau de Loubresse, N., Prokhorova, I., Holtkamp, W., Rodnina, M. V., Yusupova, G.
526 & Yusupov, M. 2014. Structural basis for the inhibition of the eukaryotic ribosome.
527 *Nature* **513**: 517, doi:10.1038/nature13737.

528 59 Friesen, W. *et al.* 2018. The minor gentamicin complex component, X2, is a potent
529 premature stop codon readthrough molecule with therapeutic potential. *Submitted for*
530 *publication*.

531 60 Taguchi, A., Hamada, K. & Hayashi, Y. 2017. Chemotherapeutics overcoming nonsense
532 mutation-associated genetic diseases: medicinal chemistry of negamycin. *J. Antibiot.* **71**:
533 205, doi:10.1038/ja.2017.112.

534 61 Blanchard, S. C., Kim, H. D., Gonzalez, R. L., Puglisi, J. D. & Chu, S. 2004. tRNA
535 dynamics on the ribosome during translation. *Proc. Natl. Acad. Sci. U. S. A.* **101**: 12893-
536 12898, doi:10.1073/pnas.0403884101.

537 62 Kizek, R., Adam, V., Hrabeta, J., Eckschlager, T., Smutny, S., Burda, J. V., Frei, E. &
538 Stiborova, M. 2012. Anthracyclines and ellipticines as DNA-damaging anticancer drugs:
539 Recent advances. *Pharmacol. Ther.* **133**: 26-39, doi:10.1016/j.pharmthera.2011.07.006.

540 63 Edwardson, D. W., Narendrula, R., Chewchuk, S., Mispel-Beyer, K., Mapletoft, J. P. J. &
541 Parissenti, A. M. 2015. Role of Drug Metabolism in the Cytotoxicity and Clinical
542 Efficacy of Anthracyclines. *Curr. Drug Metab.* **16**: 412-426,
543 doi:10.2174/1389200216888150915112039.

544 64 Lin, J., Zhou, D., Steitz, T. A., Polikanov, Y. S. & Gagnon, M. G. 2018. Ribosome-
545 Targeting Antibiotics: Modes of Action, Mechanisms of Resistance, and Implications for
546 Drug Design. *Annu. Rev. Biochem* **87**: null, doi:10.1146/annurev-biochem-062917-
547 011942.

548 65 Spahn, C. M. T., Beckmann, R., Eswar, N., Penczek, P. A., Sali, A., Blobel, G. & Frank,
549 J. 2001. Structure of the 80S Ribosome from Saccharomyces cerevisiae—tRNA-
550 Ribosome and Subunit-Subunit Interactions. *Cell* **107**: 373-386, doi:10.1016/S0092-
551 8674(01)00539-6.

552 66 Pibiri, I., Lentini, L., Melfi, R., Gallucci, G., Pace, A., Spinello, A., Barone, G. & Di
553 Leonardo, A. 2015. Enhancement of premature stop codon readthrough in the CFTR gene
554 by Ataluren (PTC124) derivatives. *Eur. J. Med. Chem.* **101**: 236-244,
555 doi:10.1016/j.ejmech.2015.06.038.

556 67 Pape, T., Wintermeyer, W. & Rodnina, M. V. 2000. Conformational switch in the
557 decoding region of 16S rRNA during aminoacyl-tRNA selection on the ribosome. *Nat.*
558 *Struct. Biol.* **7**: 104, doi:10.1038/72364.

559 68 Gromadski, K. B. & Rodnina, M. V. 2004. Streptomycin interferes with conformational
560 coupling between codon recognition and GTPase activation on the ribosome. *Nat. Struct.*
561 *Mol. Biol.* **11**: 316, doi:10.1038/nsmb742.

562 69 Cochella, L., Brunelle, J. L. & Green, R. 2006. Mutational analysis reveals two
563 independent molecular requirements during transfer RNA selection on the ribosome. *Nat.*
564 *Struct. Mol. Biol.* **14**: 30, doi:10.1038/nsmb1183.

565 70 Tsai, A., Uemura, S., Johansson, M., Puglisi, Elisabetta V., Marshall, R. A., Aitken,
566 Colin E., Korlach, J., Ehrenberg, M. & Puglisi, Joseph D. 2013. The Impact of
567 Aminoglycosides on the Dynamics of Translation Elongation. *Cell Reports* **3**: 497-508,
568 doi:10.1016/j.celrep.2013.01.027.

569 71 Zhang, J., Pavlov, M. Y. & Ehrenberg, M. 2018. Accuracy of genetic code translation
570 and its orthogonal corruption by aminoglycosides and Mg^{2+} ions. *Nucleic Acids Res.* **46**:
571 1362-1374, doi:10.1093/nar/gkx1256.

572 72 Roy, R., Hohng, S. & Ha, T. 2008. A practical guide to single-molecule FRET. *Nat.*
573 *Methods* **5**: 507, doi:10.1038/nmeth.1208.

574 73 Perez, C. E. & Gonzalez, R. L. 2011. In vitro and in vivo single-molecule fluorescence
575 imaging of ribosome-catalyzed protein synthesis. *Curr. Opin. Chem. Biol.* **15**: 853-863,
576 doi:10.1016/j.cbpa.2011.11.002.

577 74 Aitken, C. E., Petrov, A. & Puglisi, J. D. 2010. Single Ribosome Dynamics and the
578 Mechanism of Translation. *Ann. Rev. Biophys.* **39**: 491-513,
579 doi:10.1146/annurev.biophys.093008.131427.

580 75 Wang, L., Wasserman, M. R., Feldman, M. B., Altman, R. B. & Blanchard, S. C. 2011.
581 Mechanistic insights into antibiotic action on the ribosome through single-molecule
582 fluorescence imaging. *Ann. N.Y. Acad. Sci.* **1241**: E1-E16, doi:doi:10.1111/j.1749-
583 6632.2012.06839.x.

584 76 Chen, C., Zhang, H., Broitman, S. L., Reiche, M., Farrell, I., Cooperman, B. S. &
585 Goldman, Y. E. 2013. Dynamics of translation by single ribosomes through mRNA
586 secondary structures. *Nat. Struct. Mol. Biol.* **20**: 582, doi:10.1038/nsmb.2544.
587

588

589

590

591

592

593 **TABLES**

Table 1. Non-Sup Induced Readthrough

NonSup	EC_{50} (μM)	Readthrough fraction[a]	Hill n
Aminoglycosides			
Gentamicin B1	0.14 ± 0.02	0.27 ± 0.01	-
Gentamicin X2	0.42 ± 0.08	0.31 ± 0.02	-
NB124	0.52 ± 0.05	0.21 ± 0.01	-
Gentamicin B	0.54 ± 0.15	0.081 ± 0.005	-
NB84	0.68 ± 0.06	0.19 ± 0.01	-
G418	0.99 ± 0.09	0.32 ± 0.01	-
Streptothricin	1.5 ± 0.3	0.26 ± 0.01	-
Commercial Gentamicin (mixture)	4.2 ± 0.6	0.29 ± 0.02	-
Ataluren-Like			
GJ072	98 ± 4	0.16 ± 0.01	4.2 ± 0.7
RTC13	270 ± 15	0.10 ± 0.01	3.1 ± 0.5
Ataluren	350 ± 20	0.15 ± 0.01	4.3 ± 0.8
Other			
Doxorubicin	9.8 ± 1.8	0.11 ± 0.01	-
Negamycin	490 ± 70	0.13 ± 0.01	-

[a]Plateau octapeptide formed/POST5

594

595

596

597

598

599

600

601

602

603

604

FIGURES

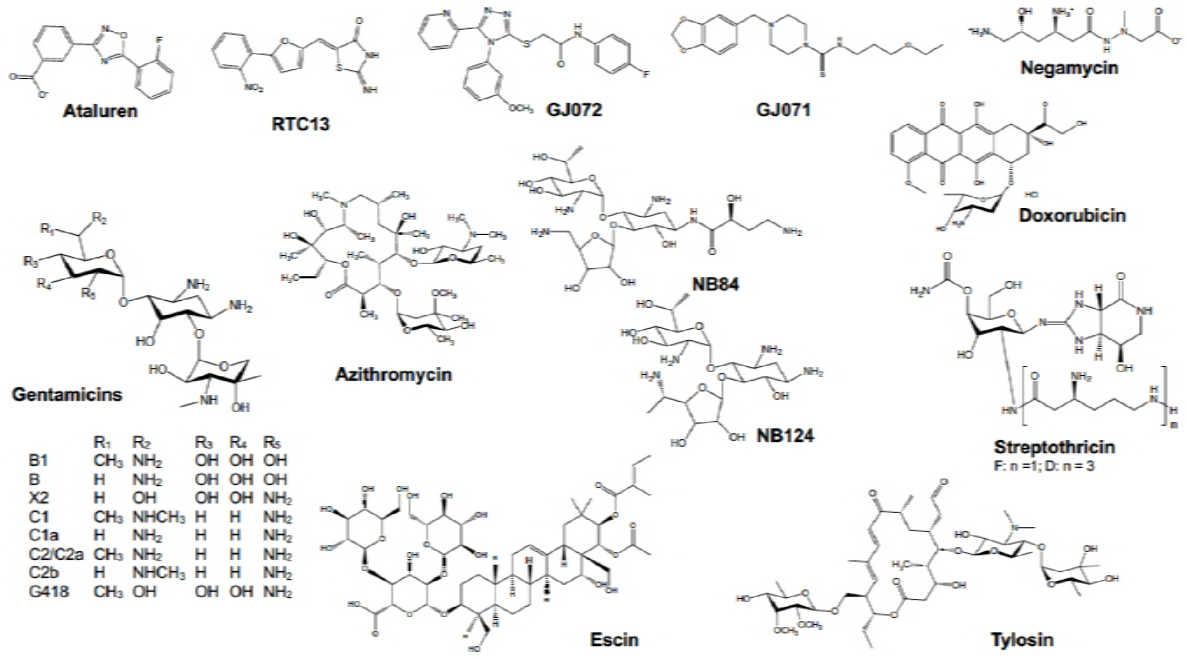

	R_1	R_2	R_3	R_4	R_5
B1	CH_3	NH_2	OH	OH	OH
B	H	NH_2	OH	OH	OH
X2	H	OH	OH	OH	NH_2
C1	CH_3	$NHCH_3$	H	H	NH_2
C1a	H	NH_2	H	H	NH_2
C2/C2a	CH_3	NH_2	H	H	NH_2
C2b	H	$NHCH_3$	H	H	NH_2
G418	CH_3	OH	OH	OH	NH_2

Figure 1. The structures of the nonsense suppressors (NonSups) studied in this work.

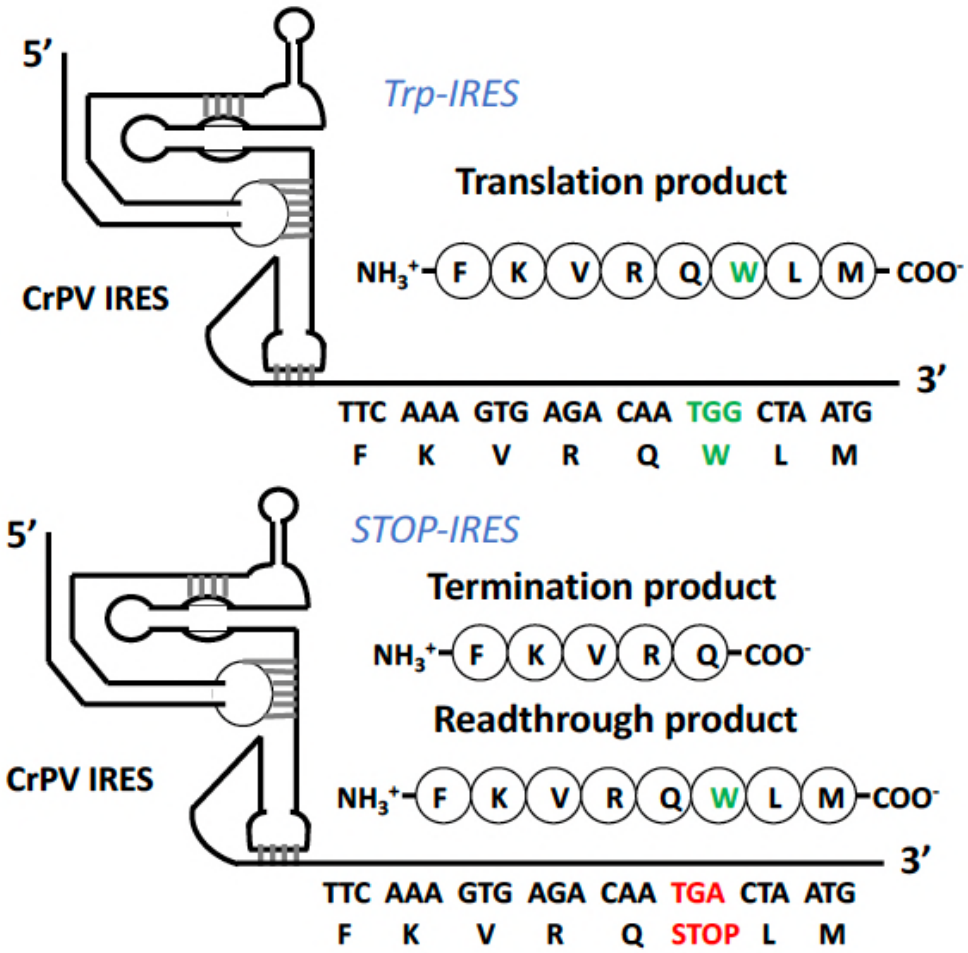

620

621 **Figure 2**. Coding sequences of Trp-IRES and Stop-IRES

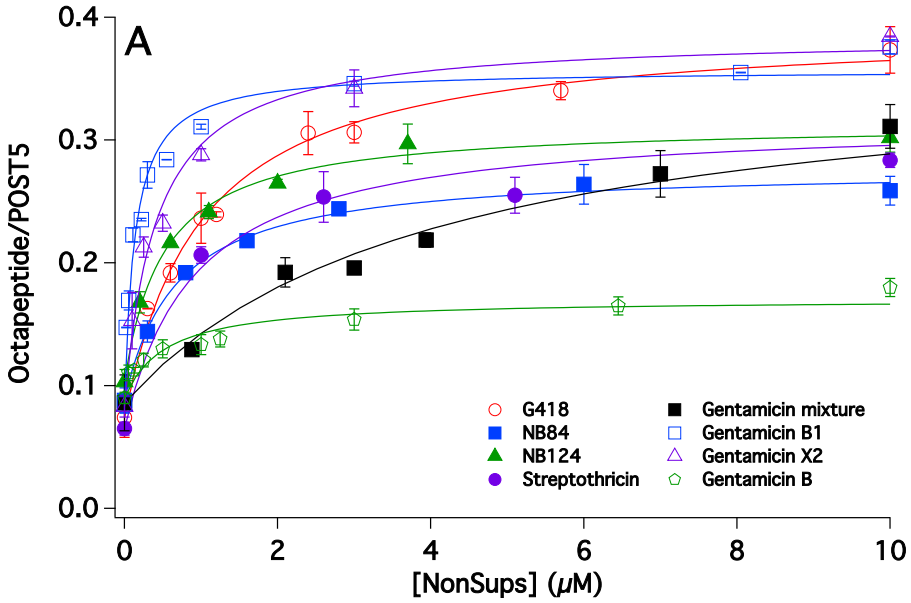

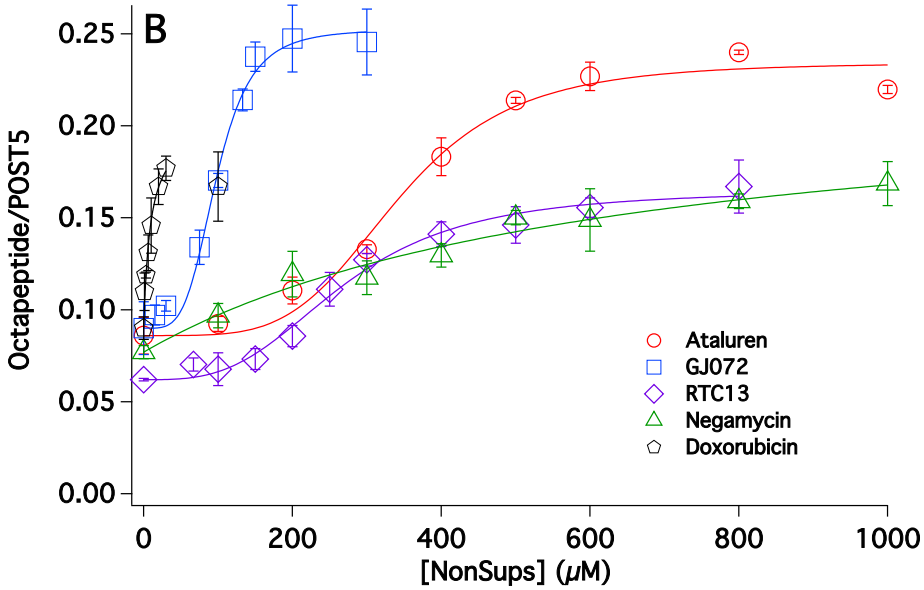

Figure 3. Readthrough as a function of nonsense suppressor concentration. A. Aminoglycosides. B. Ataluren-like NonSups and Others. The highest doxorubicin employed was 30 μM because higher concentrations led to significant ribosome and Met-tRNA^{Met} particle formation (Figure S5). None of the NonSups in Figure 3 showed appreciable inhibition of octapeptide formation from pentapeptide by ribosomes programmed with Trp-IRES at concentrations equal to twice their EC_{50} values.

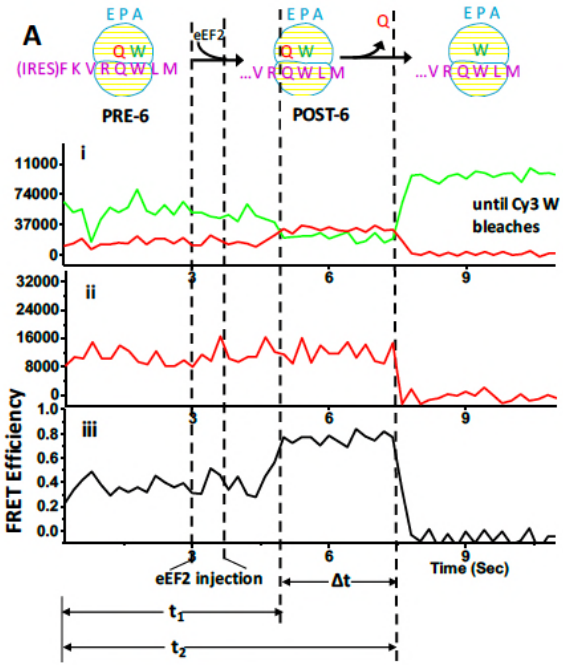

630

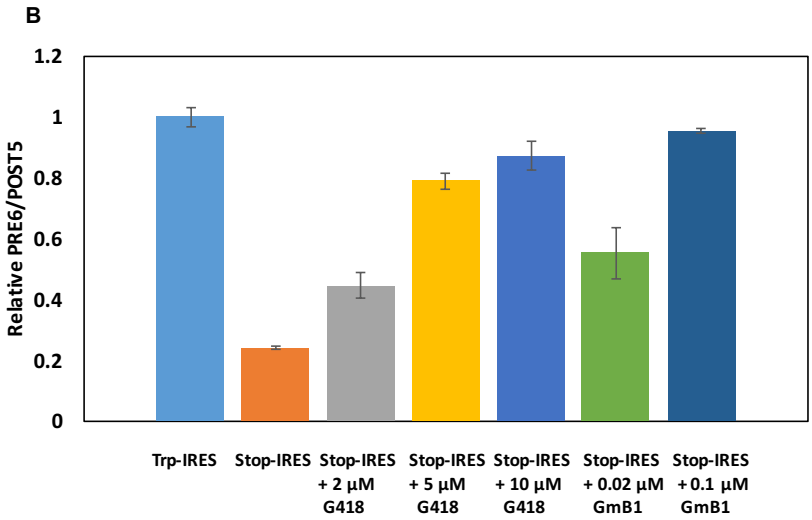

631

632 **Figure 4**. smFRET Experiments. A. eEF2-induced translocation of the 80S-Trp-IRES-PRE6
633 complex to form 80S-Trp-IRES-POST6 complex followed by release of $tRNA^{Gln}$. The Trp-IRES-
634 PRE6 complex contains $tRNA^{Gln}$(Cy5) in the P-site and FKVRQW-$tRNA^{Trp}$(Cy3) in the A-site.
635 The cartoon at top shows the state progression during translocation. i. Single molecule traces.
636 Green and red traces show $tRNA^{Trp}$(Cy3) emission and $tRNA^{Gln}$(Cy5) sensitized emission,

637 respectively, following eEF2 injection, excited at 532 nm. ii. ALEX intensity signal from direct
638 excitation of $tRNA^{Gln}$(Cy5) at 640 nm. iii. FRET efficiency between $tRNA^{Trp}$(Cy3) and
639 $tRNA^{Gln}$(Cy5) showing a transient increase following eEF2 on conversion of PRE6 complex to
640 POST6 complex. B. Dose-dependent effect of G418 and GmB1 (gentamicin B1) on PRE6
641 complex formation from 80S-Stop-IRES-POST5 complex as compared with PRE6 complex
642 formation from 80S-Trp-IRES-POST5 complex in the absence of either G418 or GmB1.
643

644 **SUPPLEMENTARY INFORMATION**

645 The tRNA-Quant and PEP-Quant assays give similar results (Figure S1).

646

647 Identification of streptothricin as a nonsense suppressor in yeast and human cells. An in-house
648 collection of 664 antimicrobial compounds was screened for suppression of two nonsense alleles
649 in *Saccharomyces cerevisiae* using a modification of a published procedure (Baradaran-Heravi*, et*
650 *al.*, 2016). Exponentially growing B0133-3B yeast cells harboring *met8-1* (TAG) and *trp5-48*
651 (TAA) nonsense alleles were seeded in 96-well plates at $A_{600} = 0.01$ in Synthetic Complete medium
652 containing 5 μM Met and 5 μM Trp. This strain is unable to grow in the presence of these low
653 concentrations of Met and Trp, unlike prototrophic strains. Antimicrobial compounds were added
654 individually to the wells using a Biorobotics TAS1 robot equipped with a 0.7 mm diameter 96-pin
655 tool, at a final concentration of ~15 μM. The plates were incubated at 30°C for 42 h and yeast
656 growth was determined by measuring A_{600}. Paromomycin was added at 10 μM to four wells as a
657 positive control. In this assay, yeast growth requires efficient suppression of both *met8-1* and *trp5-*
658 *48*. A single compound, streptothricin, enabled robust yeast growth (Figure S2A), with an EC_{50} of
659 5 μM (Figure S2B). Streptothricin was also assayed for nonsense suppression in human cells using
660 a previously described assay (Baradaran-Heravi *et al.,* 2016). Briefly, human breast carcinoma
661 HDQ-P1 cells homozygous for the *TP53* R213X (TGA) nonsense mutation were exposed to
662 different concentrations of streptothricin for 72 h and the production of full-length p53, the
663 readthrough product, and truncated p53 was determined by automated capillary electrophoresis
664 western analysis. Streptothricin showed weak readthrough activity, detectable at concentrations of
665 200 μM and above. By contrast, gentamicin B1 showed much higher levels of readthrough at lower
666 concentrations (Figure S2C).

667

668 Assay heterogeneity. The reaction mixtures used for the tRNA-Quant and Pep-Quant assays is
669 heterogeneous, with ribosomes derived from shrimp cysts or Hela cells, yeast elongation factors,
670 and yeast and *E. coli* charged tRNAs. However, such heterogeneity is not problematic. IRESs can
671 initiate translation on ribosomes from many eukaryotic organisms (Koh, *et al.*, 2014), including
672 shrimp (Cevallos and Sarnow, 2005), indicating that the molecular mechanism is not species-
673 specific. CrPV IRES can initiate translation on ribosomes from yeast (Thompson, *et al.*, 2001) to
674 human (Spahn, *et al.*, 2004). Furthermore, the structures of eukaryotic elongation factors are very
675 strongly conserved (Soares, *et al.*, 2009; Jørgensen, *et al.*, 2002), and charged tRNAs from one
676 species form fully functional complexes with both eEF1A and ribosomes from different ones
677 (Jackson, *et al.*, 2001; Ferguson, *et al.*, 2015).

678

679 Concentration dependence of Ataluren ^{19}F NMR chemical shift. A decrease in chemical shift of
680 an ^{19}F NMR peak provides an indication of molecular aggregation in solution (Iijima, *et al.*, 1999;
681 Ohta, *et al.*, 2003; Suzuki, *et al.*, 2013). We sought to determine whether aggregation was
682 responsible for the sigmoidal readthrough saturation curve for ataluren (Figure 3B) by examining
683 the chemical shift of its ^{19}F NMR peak at three concentrations, 0.03, 0.1 and 2.0 mM, that bracket
684 the range employed in the readthrough assay. We found that both the chemical shift (1.0 ppm
685 downfield from a KF standard) and the line shape of the ^{19}F NMR peak were identical at all three
686 concentrations, evidence that aggregation is unlikely to be the cause of the readthrough saturation
687 curve induced by ataluren.

688

689 NonSups having low activity in the tRNA-Quant assay (Figure S3)

690

691 Escin inhibition of octapeptide synthesis from POST-5 complexes. Escin concentrations ≥ 300 μM
692 inhibit octapeptide synthesis from POST5 complexes for ribosomes programmed with either Stop-
693 IRES (basal readthrough) or ribosomes programmed with Trp-IRES (normal octapeptide
694 synthesis), with inhibition being much more pronounced on basal readthrough (Figure S4). This
695 difference is not currently understood. One possibility under consideration is that inhibition arises
696 from a destabilization of peptidyl-tRNA binding to the A-site of a PRE6 complex, and that
697 such binding is weaker for ribosomes programmed with Stop-IRES vs. Trp-IRES.

698

699 Doxorubicin-induced particle formation by both tRNA and ribosomes. Doxorubicin
700 concentrations above 100 μM induced Met-tRNA^{Met} particle formation in accord with prior results
701 (Agudelo, *et al.*, 2016). High doxorubicin also induced particle formation by ribosome-IRES
702 complex (Figure S5). To determine the extent of particle formation, various concentrations of
703 doxorubicin were added to aliquots (250 μL) containing 0.1 μM 80S:IRES complex, 0.1 μM
704 [^{35}S]Met-tRNA^{Met}, 0.1 μM eEF1A and 1 mM GTP. The mixture was incubated at 37 °C for 20
705 min. Particles were removed by centrifugation at 17,000 X g for 25 min at 4 °C. The supernatant
706 was then layered on top of 350 μL Buffer 4 with 1.1 M sucrose and was ultracentrifuged at 540,000
707 x g for 70 min at 4°C to separate 80S-IRES from [^{35}S]Met-tRNA^{Met}. Virtually all of the A_{260} units
708 and [^{35}S] radioactivity (~98% in each case) of the low speed supernatant were found in the high
709 speed pellet and supernatant, respectively. Accordingly, measurements of A_{260} units and [^{35}S]
710 radioactivity in the low speed supernatant were used to determine the amounts of 80S-IRES and
711 [^{35}S]Met-tRNA^{Met} remaining in solution after doxorubicin-induced particle formation.

712

SUPPLEMENTARY REFERENCES

1 Baradaran-Heravi, A. *et al.* 2016. Novel small molecules potentiate premature termination codon readthrough by aminoglycosides. *Nucleic Acids Res.* **44**: 6583-6598, doi:10.1093/nar/gkw638.

2 Koh, C. S., Brilot, A. F., Grigorieff, N. & Korostelev, A. A. 2014. Taura syndrome virus IRES initiates translation by binding its tRNA-mRNA–like structural element in the ribosomal decoding center. *Proc. Natl. Acad. Sci. USA* **111**: 9139-9144, doi:10.1073/pnas.1406335111.

3 Cevallos, R. C. & Sarnow, P. 2005. Factor-Independent Assembly of Elongation-Competent Ribosomes by an Internal Ribosome Entry Site Located in an RNA Virus That Infects Penaeid Shrimp. *J. Virol.* **79**: 677-683, doi:10.1128/jvi.79.2.677-683.2005.

4 Thompson, S. R., Gulyas, K. D. & Sarnow, P. 2001. Internal initiation in *Saccharomyces cerevisiae* mediated by an initiator tRNA/eIF2-independent internal ribosome entry site element. *Proc. Natl. Acad. Sci. USA* **98**: 12972-12977, doi:10.1073/pnas.241286698.

5 Spahn, C. M. T., Jan, E., Mulder, A., Grassucci, R. A., Sarnow, P. & Frank, J. 2004. Cryo-EM Visualization of a Viral Internal Ribosome Entry Site Bound to Human Ribosomes: The IRES Functions as an RNA-Based Translation Factor. *Cell* **118**: 465-475, doi:10.1016/j.cell.2004.08.001.

6 Soares, D. C., Barlow, P. N., Newbery, H. J., Porteous, D. J. & Abbott, C. M. 2009. Structural Models of Human eEF1A1 and eEF1A2 Reveal Two Distinct Surface Clusters of Sequence Variation and Potential Differences in Phosphorylation. *PLoS One* **4**: e6315, doi:10.1371/journal.pone.0006315.

7 Jørgensen, R., Carr-Schmid, A., Ortiz, P. A., Kinzy, T. G. & Andersen, G. R. 2002. Purification and crystallization of the yeast elongation factor eEF2. *Acta Crystallogr. Sect. D. Biol. Crystallogr.* **58**: 712-715, doi:doi:10.1107/S0907444902003001.

8 Jackson, R. J., Napthine, S. & Brierley, I. 2001. Development of a tRNA-dependent in vitro translation system. *RNA* **7**: 765-773.

9 Ferguson, A. *et al.* 2015. Functional Dynamics within the Human Ribosome Regulate the Rate of Active Protein Synthesis. *Mol. Cell* **60**: 475-486, doi:10.1016/j.molcel.2015.09.013.

10 Iijima, H., Koyama, S., Fujio, K. & Uzu, Y. 1999. NMR Study of the Transformation of Perfluorinated Surfactant Solutions. *Bull. Chem. Soc. Jpn.* **72**: 171-177, doi:10.1246/bcsj.72.171.

11 Ohta, A., Murakami, R., Urata, A., Asakawa, T., Miyagishi, S. & Aratono, M. 2003. Aggregation Behavior of Fluorooctanols in Hydrocarbon Solvents. *J. Phys. Chem. B* **107**: 11502-11509, doi:10.1021/jp035134o.

12 Suzuki, Y., Brender, J. R., Soper, M. T., Krishnamoorthy, J., Zhou, Y., Ruotolo, B. T., Kotov, N. A., Ramamoorthy, A. & Marsh, E. N. G. 2013. Resolution of Oligomeric Species during the Aggregation of Aβ(1-40) Using (19)F NMR. *Biochemistry* **52**: 1903-1912, doi:10.1021/bi400027y.

13 Agudelo, D., Bourassa, P., Bérubé, G. & Tajmir-Riahi, H. A. 2016. Review on the binding of anticancer drug doxorubicin with DNA and tRNA: Structural models and antitumor activity. *J. Photochem. Photobiol. B: Biol.* **158**: 274-279, doi:10.1016/j.jphotobiol.2016.02.032.

SUPPLEMENTARY TABLES

Table S1. DMSO and MeOH each induce added basal readthrough

Volume % DMSO	Basal readthrough fraction[a] above –Trp-RNA^{Trp} background
0	0.078 ± 0.013
0.1	0.099 ± 0.004
0.33	0.12 ± 0.01
0.67	0.14 ± 0.01
1.0	0.15 ± 0.01
Volume % MeOH	
0	0.099 ± 0.012
0.17	0.10 ± 0.01
0.5	0.12 ± 0.01
1.0	0.14 ± 0.01

[a]normalized to octapeptide synthesis by Trp-IRES in the absence of either DMSO or MeOH

SUPPLEMENTARY FIGURES

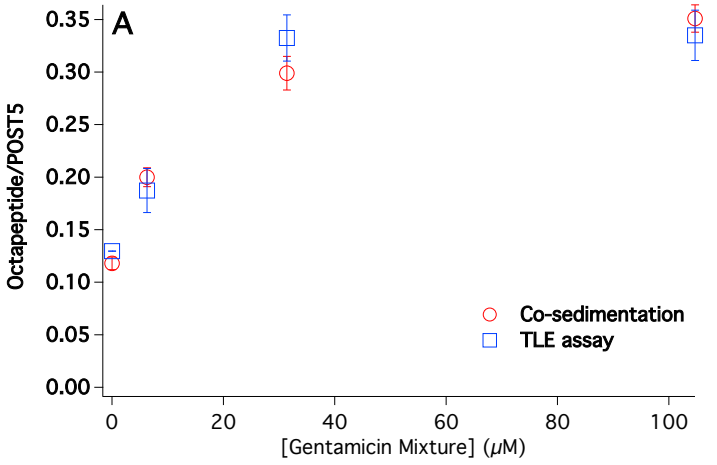

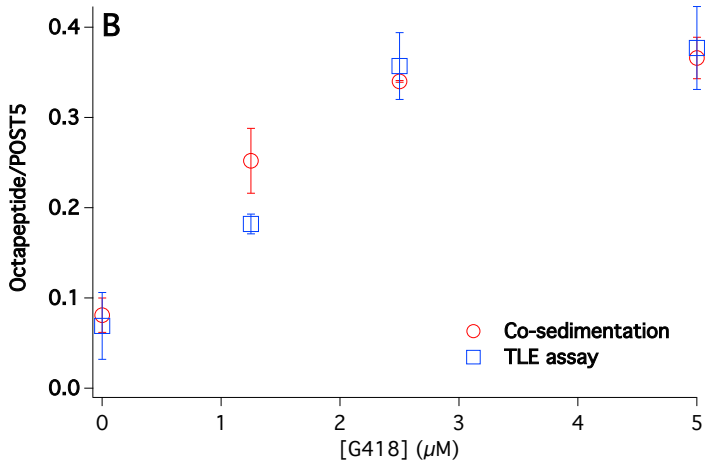

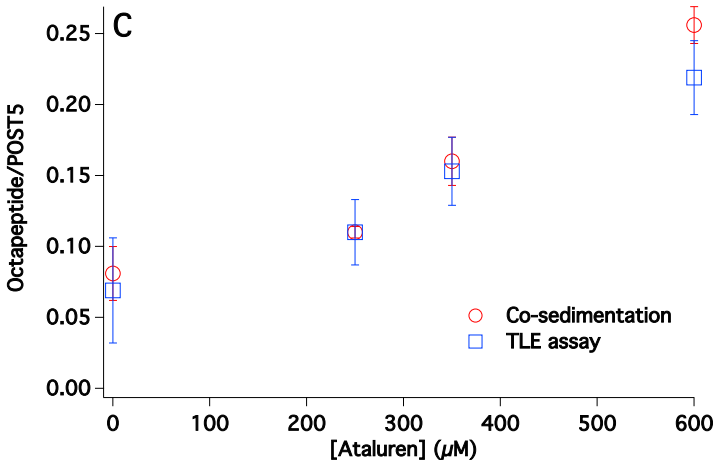

Supplementary Figure 1. tRNA-Quant vs. Pep-Quant

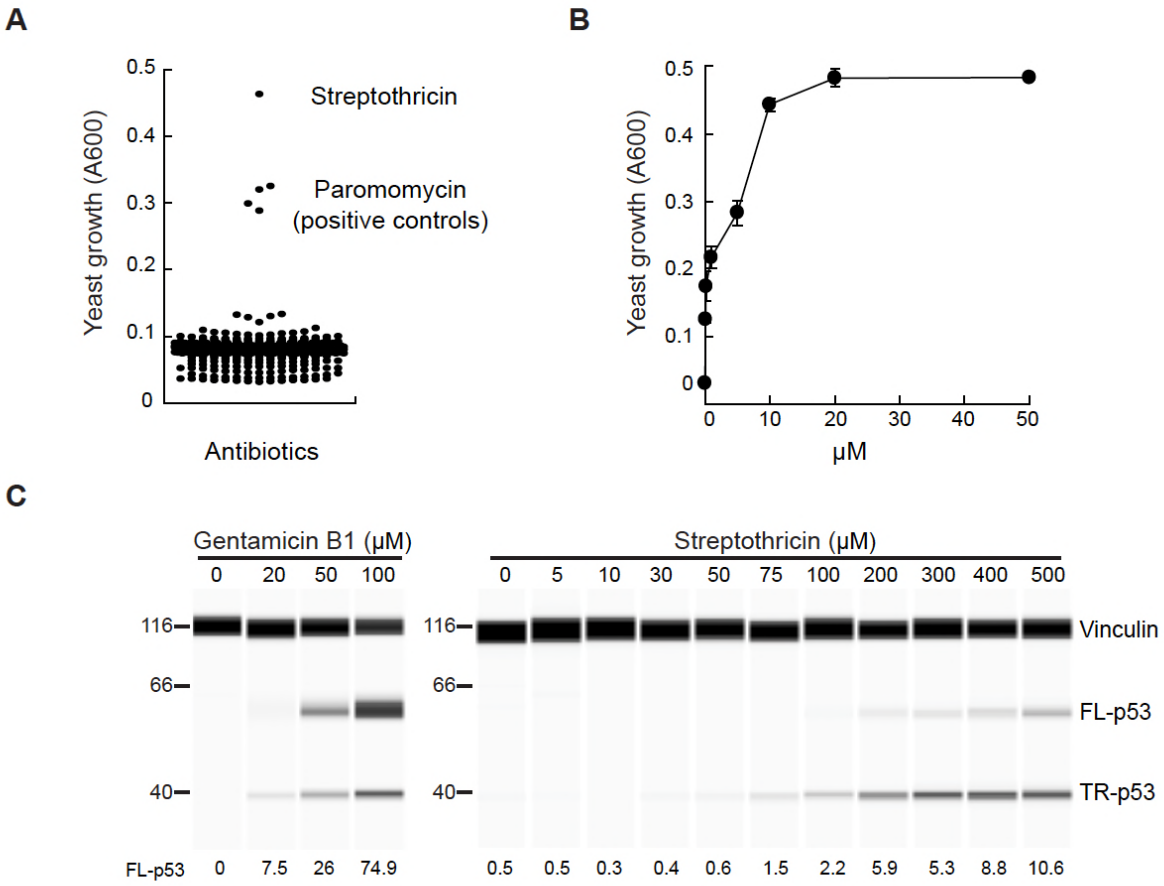

Supplemental Figure 2. Nonsense suppression by streptothricin in yeast and human cells. A. Scatter plot of the nonsense suppression activity of 664 antibiotics in yeast. B. Concentration dependence of nonsense suppression by streptothricin in yeast. C. Concentration dependence of p53 PTC readthrough in HDQ-P1 cells. Formation of full-length p53 (FL-p53) and truncated p53 (TR-p53) was determined by automated capillary electrophoresis western analysis and the results displayed as pseudoblots. FL-p53 and TR-p53 chemiluminescence signal was normalized to that of the protein loading control vinculin and expressed relative to the amount of TR-p53 detected in untreated cells.

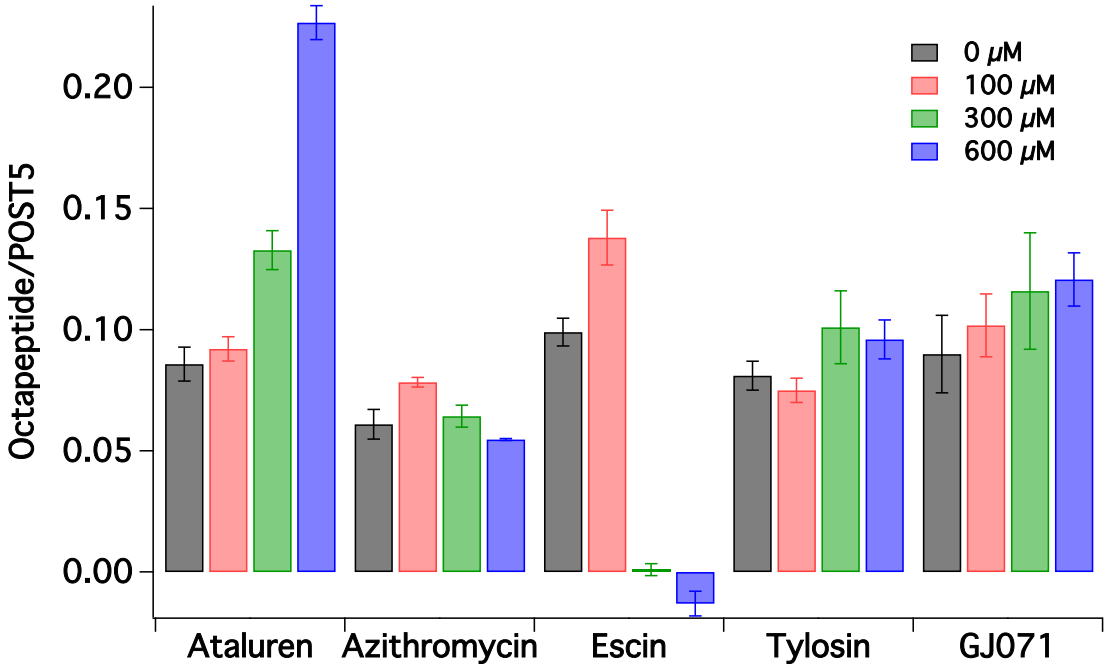

Supplementary Figure 3. Low activity NonSups. With the exception of escin (See Supplementary Figure 4), none of the NonSups in this Figure at 600 μM showed appreciable inhibition of octapeptide formation from pentapeptide by ribosomes programmed with Trp-IRES

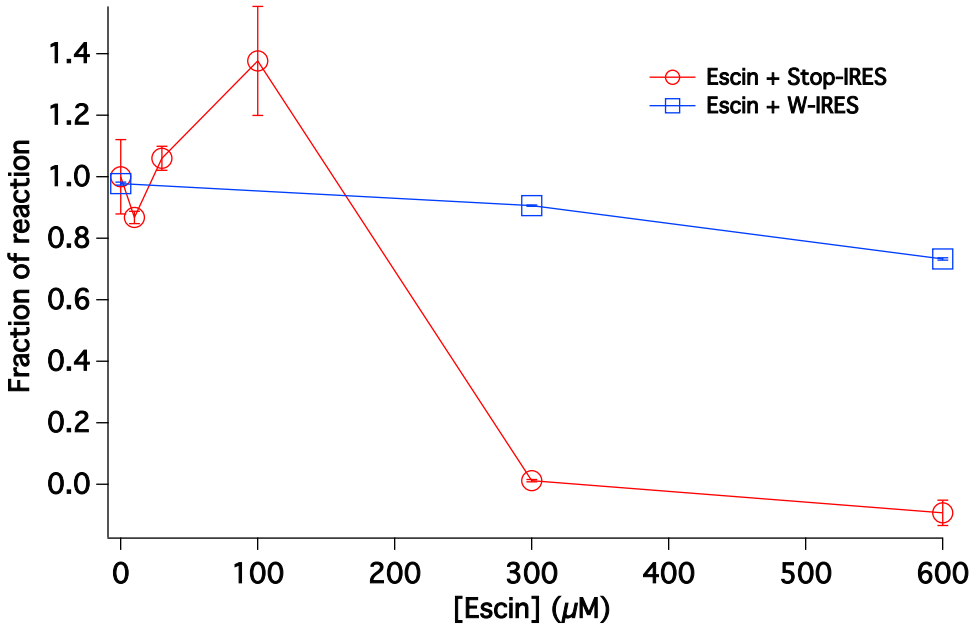

Supplementary Figure 4. High escin concentrations inhibit both basal readthrough (ribosomes programmed with Stop-IRES) and normal octapeptide synthesis (ribosomes programmed with Trp-IRES).

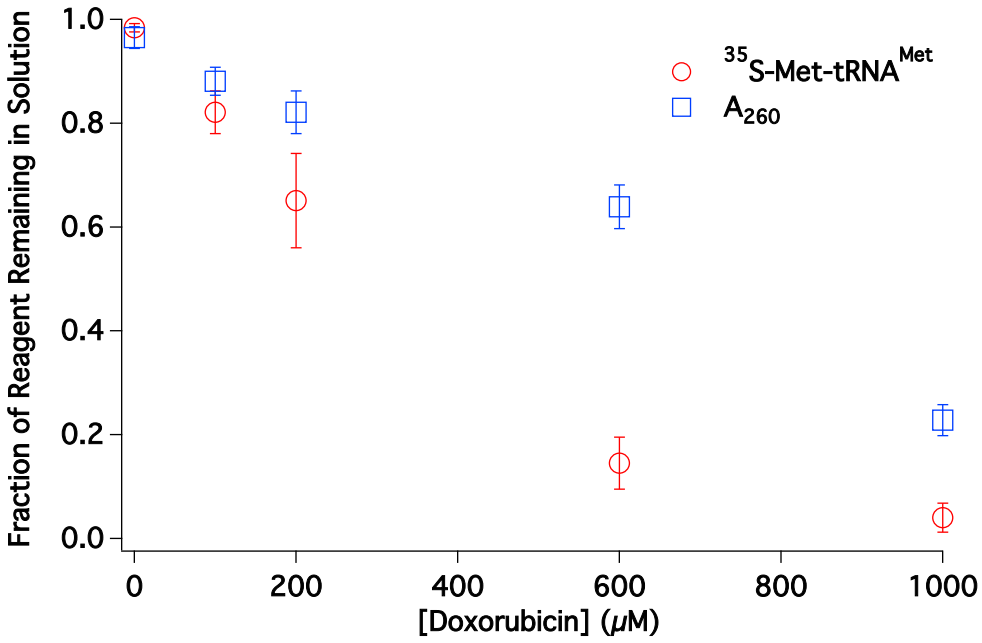

Supplementary Figure 5. High doxorubicin concentrations induce particle formation by both Met-tRNA^{Met} and 80S-IRES complexes.